JURNAL KIMIA VALENSI
p-ISSN: 2460-6065; e-ISSN: 2548-3013
Journal homepage: https://journal.uinjkt.ac.id/index.php/valensi
Research Article

Hydrothermal Growth of Titanium Dioxide Thin Films on Conductive Substrates: Insights into Optical Properties

Yulia Eka Putri[1*], Tio Putra Wendari[1], Retno Dyah Wulandari[1], Melvi Muharmi[2], Mai Efdi[1], Refinel Refinel[1]

[1]*Department of Chemistry, Faculty of Mathematics and Natural Sciences, Universitas Andalas, Padang (25163), Indonesia*
[2]*Chemical Analyst Study Program, Department of Mathematics and Natural Sciences, Faculty of Science and Technology, Universitas Jambi, Muaro Jambi. 35361, Indonesia*

[*]*Email: yuliaekaputri@sci.unand.ac.id*

Article Info
Received: Sept 26, 2025
Revised: Oct 1, 2025
Accepted: Nov 24, 2025
Online: Dec 22, 2025

Citation:
Putri, Y. E., Wendari, T. P., Wulandari, R. D., Muharmi, M., Efdi, M., Refinel, R. (2025). Hydrothermal Growth of Titanium Dioxide Thin Films on Conductive Substrates: Insights into Optical Properties. *Jurnal Kimia Valensi*, 11(2), 284-290.

Doi: 10.15408/jkv.v11i2.46532

Abstract
Titanium dioxide (TiO_2) thin films were deposited on fluorine-doped tin oxide (F:SnO_2/FTO) conducting glass using the hydrothermal method. The X-ray diffraction (XRD) patterns confirmed that the TiO_2 thin films crystallize in the rutile phase, exhibiting high crystallinity. The Fourier Transform Infrared (FTIR) spectrum confirmed the interaction between the FTO substrate and the TiO_2 layer, indicated by an absorption peak in the range of 400 cm^{-1} to 900 cm^{-1}. These peaks correspond to Ti–O–Ti and Ti–O vibrations within the octahedral structure of TiO_6 and Sn–O–Ti vibrations, indicating the bonding between the FTO substrate and the TiO_2 surface. Scanning Electron Microscopy (SEM) images provide detailed visualization of the morphological features of the TiO_2 thin films deposited on FTO glass, as evidenced by the prolonged hydrothermal processing resulting in the formation of thicker films. In addition, the interface between the TiO_2 layer and the FTO substrate is well-defined and continuous. UV-Visible Diffuse Reflectance Spectroscopy (UV-Vis DRS) analysis showed enhanced light absorption with increasing film thickness, which was also visually noticeable. As a result, the band gap energy decreases with increasing thickness, indicating that less energy is required to excite electrons from the valence band to the conduction band.

Keywords: Hydrothermal, rutile, thin film, TiO_2

1. INTRODUCTION

Nanotechnology represents a cutting-edge realm involving materials scaled down to dimensions ranging from 1 to 100 nanometers, exhibiting unique chemical and physical properties superior to bulk materials [1]. Nanomaterials are categorized based on their dimensions into 1D, 2D, and 3D structures, with 2D nanomaterials currently garnering significant attention for their potential in nanotechnological innovations [2]. Among these dimensions, 2D thin films stand out as a prominent example. The development of 2D thin films aims to harness materials with advanced functionalities, including transistors [3], photocatalysts [4], coatings for self-cleaning [5], batteries [6], sensors [7], and implants [8].

One of the 2D compounds that has attracted attention as a thin film is titanium dioxide (TiO_2). TiO_2 is gaining attention as a promising material for thin films due to its semiconductor properties, high surface area and surface reactivity, thermal stability, non-toxicity, eco-friendliness, and abundance in nature. It has demonstrated excellent performance in various applications such as photocatalysis, dye degradation, solar cells, self-cleaning surfaces, smart windows, anti-fogging coatings, and photochromic materials [9]. TiO_2 thin films can be deposited on both non-conductive substrates like glass and conductive substrates, such as indium tin oxide (ITO), fluorine tin oxide (FTO), silicon wafers, and metal oxides. Studies have reported that the presence of tin oxide (SnO_2) layer on the glass substrate serves as a favorable

nucleation site during the growth of TiO_2 [10]. FTO glass stands out as a highly efficient substrate choice due to its excellent chemical and thermal stability, superior mechanical strength, and cost-effectiveness. Moreover, the optical characteristics of the TiO_2 thin film on the FTO glass substrate exhibit significant UV-Vis absorption capabilities, rendering it a promising contender for harnessing solar photons in photoelectrochemical applications [11].

A number of methods have been utilized to produce TiO_2 thin films, including physical techniques such as dip coating, chemical vapor deposition (CVD), physical vapor deposition (PVD), pulsed laser deposition (PLD), and magnetron sputtering, as well as chemical methods like electrochemistry and hydrothermal synthesis. Among these, the hydrothermal method stands out for its simplicity, relatively low synthesis temperature, and equipment accessibility, making it suitable for thin film fabrication on specific substrates [12]. Therefore, in this study, we employed the hydrothermal technique to synthesize TiO_2 thin films on FTO substrates with varying synthesis times. Variation in synthesis time affects parameters such as crystal growth, particle size, film thickness, and surface morphology, which in turn affect the structural and optical properties of the resulting thin films. Therefore, optimizing the deposition process and obtaining films with desired crystallinity and thickness play a crucial role in determining their functional properties. Furthermore, FTO substrates were chosen for their long-term stability, high mechanical strength, good film adhesion under normal and high-temperature conditions, and the requirement for a flat and smooth surface to prevent chemical reactions from altering film properties. The resulting TiO_2 thin films were characterized to investigate their crystal structure, surface interactions, and optical properties.

2. RESEARCH METHODS

The materials used in this study included titanium (IV) butoxide (TBOT) from Sigma-Aldrich, ethanol from Merck, hydrochloric acid 36.5~38% (HCl) from Merck, deionized water, and FTO glass. All materials were utilized without undergoing further purification, and the dimension of FTO glass used in the samples varies in length and width; however, all samples have the same FTO thickness of 3 mm. The equipment utilized for characterization were: X-Ray Diffraction (XRD-PANalytical), Fourier Transform Infrared (FTIR-PerkinElmer), Scanning Electron Microscope (SEM-Carl Zeiss EXO 10), and Diffuse Reflectance Spectroscopy UV-Vis (DRS UV-Vis-Analytik Jena Specord 210).

FTO substrates were prepared by rinsing and sonicating in distilled water and ethanol for 15 minutes each, followed by air-drying the clean FTO glass. For the TiO_2 solution preparation, 17.1428 mL of 37% HCl was dissolved in 17.1428 mL of deionized water with stirring for 10 minutes. Once the solution became homogeneous, 0.7143 mL of titanium (IV) butoxide was added dropwise while stirring for an additional 10 minutes. The resulting clear solution was then transferred into a Teflon-lined autoclave. Subsequently, the FTO glass was positioned vertically within the autoclave. The hydrothermal process was conducted at 150 °C for durations of 3, 5, and 8 hours. After the hydrothermal treatment, the TiO_2-coated substrate was dried at room temperature. The TiO_2 thin film samples were designated as TLF-3, TLF-5, and TLF-8, respectively. Characterization of the TiO_2 thin films was carried out using XRD, FTIR, SEM, and DRS UV-Vis.

3. RESULTS AND DISCUSSION

Hydrothermal synthesis of TiO_2 thin films used titanium (IV) butoxide (TBOT) as the Ti precursor, hydrochloric acid (HCl) as the catalyst, and deionized water as the solvent. The synthesis involved varying synthesis times of 3 hours, 5 hours, and 8 hours on an FTO glass substrate. The visual appearance of the post-synthesis samples is shown in **Figure 1**. The FTO size differed among the samples, resulting in varying surface areas for deposition; however, this variation did not affect the synthesis process, particularly during the nucleation and crystal growth stages. As the hydrothermal reaction time increases, the TiO_2 film becomes thicker due to the higher particle density. Extended synthesis times promote grain growth and improve crystallinity, which helps reduce lattice defects and lowers the band gap energy. Subsequently, the synthesis duration affects not only the film thickness and transparency but also its structural order and optical characteristics [13].

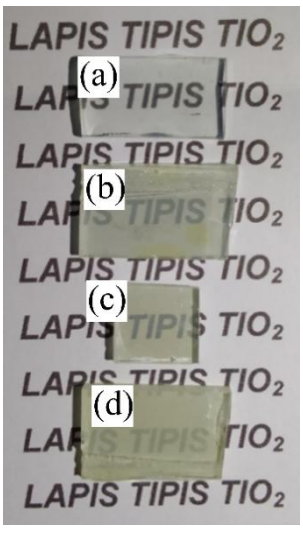

Figure 1. The physical appearance of the TiO_2 thin film samples. (a) FTO glass substrate, (b) TLF-3, (c) TLF-5, and (d) TLF-8

The reaction mechanism for TiO_2 formation initiates with a hydrolysis process in an acidic environment. Here, the lone electron pair of the oxygen atom in titanium butoxide interacts with a hydrogen ion from the hydronium ion, generating the oxygen atom to have a positive charge, resulting electron deficiency. Subsequently, the lone electron pair of the oxygen atom in a water molecule attacks the titanium atom, leading to the release of butanol and the formation of titanium hydroxide ($Ti(OH)_4$). Next, the lone pair of electrons on the oxygen atom within the Ti–OH bond reacts with a hydrogen atom from hydrochloric acid (HCl), generating a protonated oxygen atom. This protonated oxygen atom is further deprotonated with the assistance of the chloride ion, which facilitates the condensation process and results in the formation of water molecules. Finally, this condensation process finishes in the creation of TiO_2 compounds (controlled structure and growth mechanism [14]. The synthesis reactions can be explained as follows:

Hydrolysis

$$Ti(OC_4H_9)_4 + 4H_2O \rightarrow Ti(OH)_4 + 4C_4H_9OH$$

Dehydration

$$Ti(OH)_4 + Ti(OH)_4 \rightarrow TiO_2 + 2H_2O$$

The XRD patterns of the TiO_2 thin film, as shown in **Figure 2**, show the peak positions and relative intensities of the TiO_2 crystal structure compared with the standard ICSD database. The XRD pattern reveals diffraction peaks at 2θ angles of 27.43°, 36.17°, 41.27°, 54.44°, and 62.80° with corresponding hkl values of (110), (101), (111), (211), and (002), respectively. These peaks signify that the TiO_2 thin layer is in the rutile phase, possessing a tetragonal structure (ICSD #109469). Additionally, the XRD pattern exhibits diffraction peaks corresponding to SnO_2 in all three samples (ICSD #157448) as the substrate [15]. In the TLF-3 sample, the intensity of the SnO_2 diffraction peak surpasses that of the TiO_2; however, the peak intensity of the TiO_2 at the (110) crystal plane increases further in samples TLF-5 and TLF-8. This increase suggests that the thermal energy during the hydrothermal process is insufficient for substantial growth of the TiO_2 layer on the FTO glass substrate, indicating that the TiO_2 layer formed on the TLF-3 sample remains too thin [16]. Conversely, the SnO_2 diffraction peak in samples TLF-5 and TLF-8 exhibits lower intensity compared to the TiO_2 peak. This observation implies that the extended duration in the hydrothermal process provides additional energy to TiO_2 atoms, facilitating complete crystal growth and enhancing the arrangement of crystal planes.

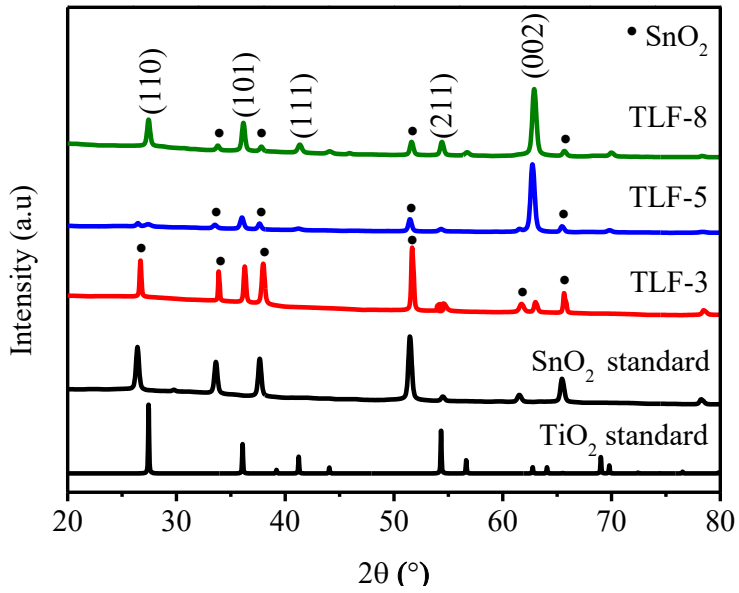

Figure 2. The XRD patterns of the TiO_2 thin film samples

The FTIR spectrum displayed in **Figure 3** provides the identification of functional groups in the TiO_2 thin films by analyzing peaks associated with particular vibrational modes. The results do not exhibit significant differences in peak patterns for TiO_2 thin films synthesized with varying hydrothermal process times. The absorption peaks within the range of 400 cm^{-1} to 900 cm^{-1} were attributed to the presence of TiO_6 octahedra, indicating the formation of TiO_2 compound. The weak absorption peak at 1100 cm^{-1} indicates the stretching vibration of the silanol and siloxane groups, originating from the glass substrate. The peaks in the range of 400 to 500 cm^{-1} can be ascribed to the stretching and bending modes of Ti-O-Ti in all three TiO_2 samples [17]. Moreover, the vibration mode observed at 560 cm^{-1} indicates the interaction

between Ti–O–Ti and Sn-O-Ti, implying a potential interaction between SnO_2 and the TiO_2 thin film [18,19]. The Si–O stretching vibration detected in the FTIR spectrum likely originates from the underlying silica glass substrate. This vibration does not indicate a direct chemical reaction affecting the TiO_2 deposition process but rather reflects the substrate's inherent composition. However, during the hydrothermal synthesis, limited interfacial diffusion of Si species into the TiO_2 layer may occur, potentially enhancing interfacial bonding and adhesion between the film and the substrate. Such interdiffusion can improve film stability without significantly altering the TiO_2 lattice structure.

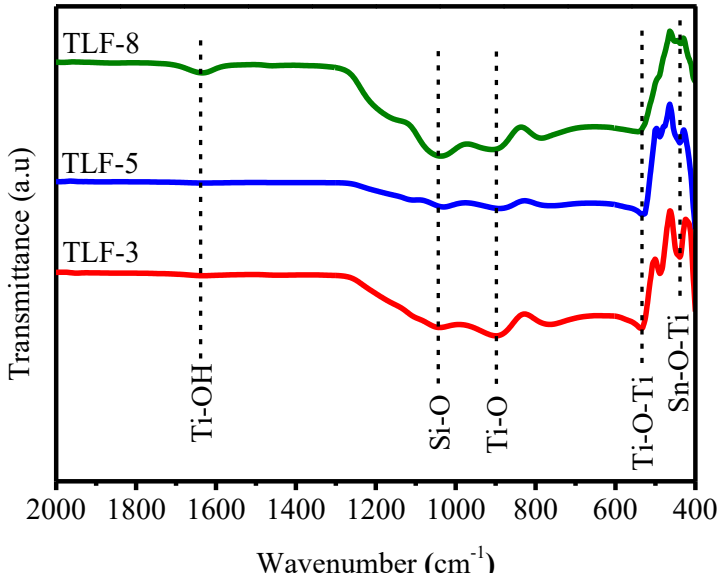

Figure 3. The FTIR spectrum of the TiO_2 thin film samples

SEM image analysis confirms the successful formation of TiO_2 on the FTO substrate via the hydrothermal method. The images shown in **Figure 4** provide valuable insights into the structural and morphological characteristics of TiO_2 thin films deposited on FTO glass substrates via the hydrothermal method. Morphological characterization was carried out on TLF-8 sample, as XRD analysis showed that this sample exhibited diffraction peaks with the highest intensity. In contrast, the TLF-3 and TLF-5 samples showed weaker diffraction patterns. **Figure 4(a)** shows a cross-sectional view of the FTO glass, clearly showing a uniform and smooth layer with a measured thickness of approximately 900 nm, and **Figure 4(b)** displays the top view of the smooth and compact surface, indicating the regularities of FTO particles. A cross-sectional image of the TLF-8 sample (**Figure 4(c)**) shows a thick TiO_2 layer deposited on the FTO substrate. The TiO_2 layer is measured to be around 15 µm, indicating substantial film growth with a dense structure. The interface between the TiO_2 and FTO is distinct but continuous, suggesting good adhesion between the two layers, as evidenced by an absorption band at 560 cm^{-1} in the FTIR spectrum. The top-view image (**Figure 4(d)**) shows a textured, rough, and uneven surface, with visible grains and possible agglomerates, indicating a non-uniform but continuous deposition of TiO_2 over the substrate.

The analysis conducted using Diffuse Reflectance Spectroscopy UV-Vis aims to ascertain the band gap energy of semiconductor materials when exposed to UV light. The optical absorption measurements using DRS UV-Vis, conducted within the wavelength range of 300–400 nm for all samples as depicted in Figure 5 (inset), show absorption peaks in the ultraviolet wavelength region. Within this range, the resulting TiO_2 thin layer tends to absorb most incoming light, resulting in high absorption values [20]. The prepared samples of TLF-3, TLF-5, and TLF-8 demonstrate that as the hydrothermal time increases, the thickness of the layer visibly increases, resulting in reduced transparency. This phenomenon occurs because thicker layers grown on the glass substrate possess a higher density of constituent atoms, leading to increased photon collisions and greater difficulty for light rays to penetrate through [21].

The Eg value was estimated by a classical extrapolation approach according to: $(\alpha h\upsilon) = \beta (h\upsilon - Eg)^{1/2}$, where α is the absorption coefficient being a fuction of wavelength (cm^{-1}), *h* is the Planck's constant (J.s), υ is the frequency of the photon energy, β is a constant, and Eg is the band gap energy (eV). As shown in **Figure 5**, the samples TLF-3, TLF-5, and TLF-8 exhibit band gap energy values, namely 3.11

eV, 3.14 eV, and 3.05 eV, respectively. This suggests a correlation between the absorption value and the resulting band gap energy [22]. According to the Tauc Plot method formula, the absorption is inversely proportional to the band gap energy value, indicating that higher absorption values correspond to smaller band gap energies. A smaller band gap energy implies that lower energy is required to excite electrons from the valence band to the conduction band, a consequence of the increased thickness of the TiO_2 thin layer produced via the hydrothermal process [23].

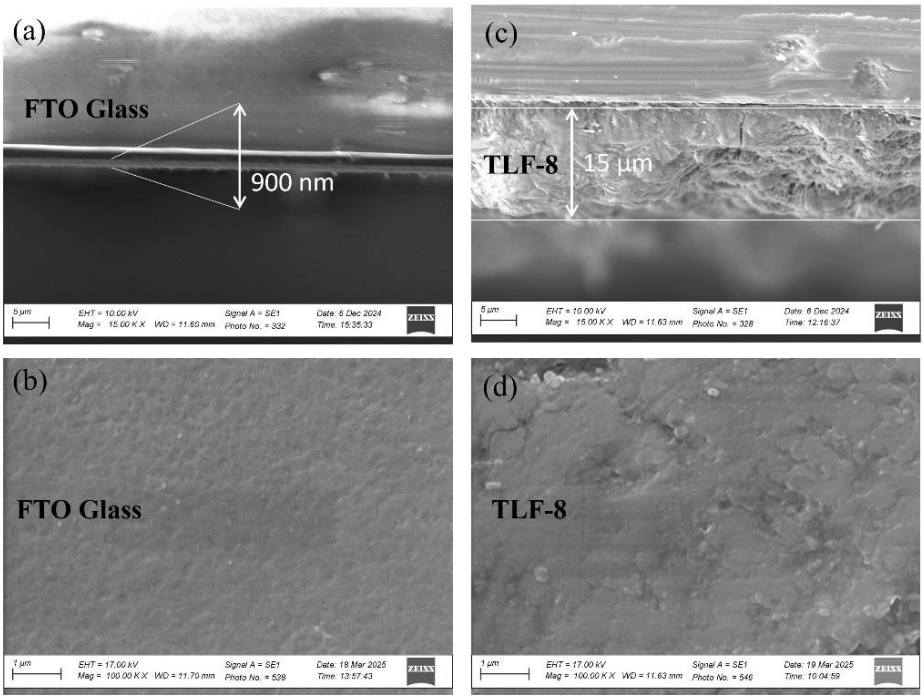

Figure 4. SEM images of TiO_2 thin film samples, (a,c) cross-section, and (c,d) surface of the pellet samples

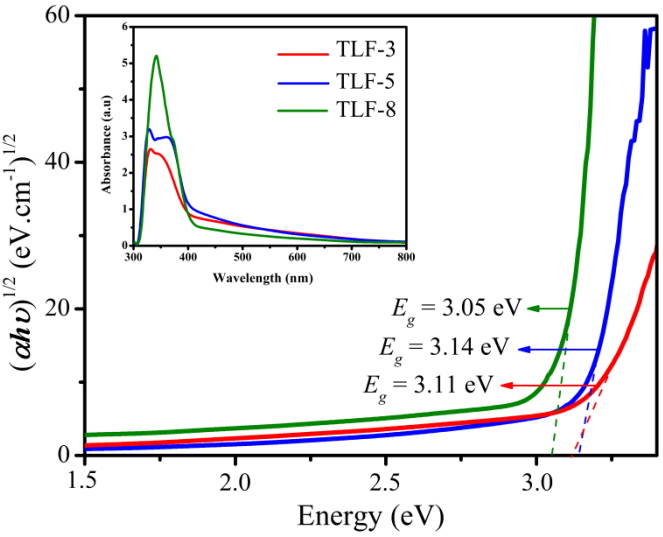

Figure 5. (a) DRS absorption region of the TLF samples, and (b) the plots of $(\alpha h\upsilon^{1/2})$ vs $h\upsilon$ for the determination of the optical band gap of TiO_2 thin film

Furthermore, the Eg values of all samples are nearly identical to the band gap energy of rutile phase TiO_2 in bulk form, which is 3.02 eV. This suggests that the TLF-3 and TLF-5 samples are still outside the nanometer thickness range. The optical properties may degrade when the film thickness exceeds the nanometer scale, as a result of enhanced light absorption and scattering, which reduces transparency. Furthermore, excessive thickness can influence the crystallinity, ultimately leading to a decline in the overall structural quality of the film. The strong interface bonding and substantial film thickness

indicate that the hydrothermal method is potentially suitable for scalable thin film fabrication.

The TLF-5 sample exhibits the highest band gap value (3.14 eV), which can be attributed to incomplete crystal growth. Such structural features lead to localized lattice disorder and possible quantum confinement effects, both of which contribute to a widening of the band gap value. In contrast, the TLF-8 sample, which possesses greater thickness and improved crystallinity, shows a smaller band gap (3.05 eV), approaching the value of bulk rutile TiO_2 (3.02 eV). This trend explains that as the film becomes thicker and more structurally ordered, the band gap narrows due to reduced lattice defects.

4. CONCLUSIONS

The synthesis of TiO_2 thin films via the hydrothermal method at 150 °C with different heating durations of 3, 5, and 8 hours, leading to the formation of the rutile phase. This interpretation is supported by the XRD pattern analysis, which shows peak correspondence with the standard rutile phase of TiO_2. Additionally, the XRD pattern indicated that the TLF-8 sample exhibited higher crystallinity compared to the TLF-3 and TLF-5 samples. The FTIR spectrum revealed the interaction between the FTO substrate and the TiO_2 thin layer through specific absorption features. Furthermore, UV–Vis DRS analysis confirmed that increasing the film thickness enhances its light absorption. UV–Vis DRS analysis confirmed that increasing the film thickness enhances its light absorption, which aligns with visual observations; as a result, the band gap energy values of the samples demonstrate a decreasing trend. A smaller band gap energy implies a lower energy requirement for exciting electrons from the valence band to the conduction band. This phenomenon is attributed to the greater film thickness of the TLF-8 sample synthesized via hydrothermal processing, as evidenced by the SEM images.

ACKNOWLEDGMENTS

This work was financially supported by the Ministry of Education, Culture, Research, and Technology of the Republic of Indonesia and the Research Institute and Community Service of Universitas Andalas through a research grant of Penelitian Dasar Unggulan Klaster Riset–Publikasi Percepatan Ke Guru Besar (Grant No T/16/UN16.19/IS-PDU-KRP2GB-Unand/2023)

REFERENCES

1. Baig N, Kammakakam I, Falath W, Kammakakam I. Nanomaterials: A review of synthesis methods, properties, recent progress, and challenges. *Mater Adv*. 2021;2(6):1821-1871. doi:10.1039/d0ma00807a
2. Catania F, De Souza Oliveira H, Lugoda P, Cantarella G, Münzenrieder N. Thin-film electronics on active substrates: Review of materials, technologies and applications. *J Phys D Appl Phys*. 2022;55(32). doi:10.1088/1361-6463/ac6af4
3. Samanta C, Yuvaraja S, Zhama T, Zhao H, Gundlach L, Zeng Y. High-performance TiO_2 thin film transistors: In-depth investigation of the correlation between interface traps and oxygen vacancies. *[supplementary information]*.
4. Alotaibi AM, Promdet P, Hwang GB, Li J, Nair SP, Sathasivam S, Kafizas A, Carmalt CJ, Parkin IP. Zn and N codoped TiO_2 thin films: Photocatalytic and bactericidal activity. *ACS Appl Mater Interfaces*. 2021;13(8):10480-10489. doi:10.1021/acsami.1c00304
5. Shabrina N, Salsabila NK, Sudarsono S, Yudoyono G. Characterization of the structure, morphology, and optical properties of titanium dioxide thin film deposited by spray pyrolysis technique for self-cleaning glass. *J Phys Conf Ser*. 2024;2780(1):012020. doi:10.1088/1742-6596/2780/1/012020
6. Oukassi S, Baggetto L, Dubarry C, Le Van-Jodin L, Poncet S, Salot R. Transparent thin film solid-state lithium ion batteries. *ACS Appl Mater Interfaces*. 2019;11(1):683-690. doi:10.1021/acsami.8b16364
7. Sun Z, huang L, Zhang Y, Wu X, Zhang M, Liang J, Bao Y, Xia X, Gu H, Homewood K, Lorenco M, Gao Y. Homojunction TiO_2 thin film-based room-temperature working H2 sensors with non-noble metal electrodes. *Sens Actuators B Chem*. 2024;398:134675. doi:10.1016/j.snb.2023.134675
8. Rajan ST, Arockiarajan A. Thin film metallic glasses for bioimplants and surgical tools: A review. *J Alloys Compd*. 2021;876:159939. doi:10.1016/j.jallcom.2021.159939
9. Haider AJ, Jameel ZN, Al-Hussaini IHM. Review on: Titanium dioxide applications. *Energy Procedia*. 2019;157:17-29. doi:10.1016/j.egypro.2018.11.159
10. Sadhu S, Jaiswal A, Adyanthaya S, Poddar P. Surface chemistry and growth mechanism of highly oriented, single crystalline TiO_2 nanorods on transparent conducting oxide coated glass substrates. *RSC Adv*. 2013;3(6):1933-1940. doi:10.1039/C2RA21516K
11. Kite SV, Sathe DJ, Patil SS, Bhosale PN, Garadkar KM. Nanostructured TiO_2 thin films by chemical bath deposition method for high

photoelectrochemical performance. *Mater Res Express*. 2019;6(2). doi:10.1088/2053-1591/aaed81

12. Salleh F, Usop R, Saugi NS, Salih EY, Mohamad M, Ikeda H, Sabri MFM, Ahmad MK, Said SM. Influence of TiO_2 layer's nanostructure on its thermoelectric power factor. *Appl Surf Sci*. 2019;497:143736. doi:10.1016/j.apsusc.2019.143736
13. Khizir H, Abbas T. Hydrothermal growth and controllable synthesis of flower-shaped TiO2 nanorods on FTO coated glass. *Journal of Sol-Gel Science and Technology*. 2021;98(3) (2021):487-496. doi:10.1007/s10971-021-05531-z
14. Prathan A, Sanglao J, Wang T, Bhoomanee C, Ruankham P, Gardchareon A, Wongratanaphisan D. Controlled structure and growth mechanism behind hydrothermal growth of TiO_2 nanorods. *Sci Rep*. 2020;10(1):1-12. doi:10.1038/s41598-020-64510-6
15. Shilpa G, Mohan Kumar P, Kishore Kumar D, Deepthi PR, Sukhdev A, Bhaskar P. A rutile phase-TiO_2 film via a facile hydrothermal method for photocatalytic methylene blue dye decolourization. *Mater Today Proc*. 2022;5477-5482. doi:10.1016/j.matpr.2022.04.148
16. Gupta T, Samriti, Cho J, Prakash J. Hydrothermal synthesis of TiO_2 nanorods: formation chemistry, growth mechanism, and tailoring of surface properties for photocatalytic activities. *Mater Today Chem*. 2021;20:100428. doi:10.1016/j.mtchem.2021.100428
17. Senthamarai R, Ramakrishnan VM, Palanisamy B, Kulandhaivel S. Synthesis of TiO_2 nanostructures by green approach as photoanodes for dye-sensitized solar cells. *Int J Energy Res*. 2021;45(2):3089-3096. doi:10.1002/er.6002
18. Zhang B, Tian Y, Zhang JX, Cai W. Structural, optical, electrical properties and FTIR studies of fluorine doped SnO_2 films deposited by spray pyrolysis. *J Mater Sci*. 2011;46(6):1884-1889. doi:10.1007/s10853-010-5021-3
19. Orozco-Gonzalez LR, Acosta-Najarro DR, Magaña-Zavala CR, Tavizon-Pozos JA, Cervantes-Cuevas H, Chavez-Esquivel G. Photocatalytic degradation of naproxen using single-doped TiO2/FTO and co-doped TiO_2-VO_2/FTO thin films synthesized by sonochemistry. *Int J Chem React Eng*. 2023;21(4):493-510. doi:10.1515/ijcre-2022-0109
20. Taherniya A, Raoufi D. Thickness dependence of structural, optical and morphological properties of sol-gel derived TiO_2 thin film. *Mater Res Express*. 2018;6(1):016417. doi:10.1088/2053-1591/aae4d0
21. Manickam K, Muthusamy V, Manickam S, Senthil TS, Periyasamy G, Shanmugam S. Effect of annealing temperature on structural, morphological and optical properties of nanocrystalline TiO_2 thin films synthesized by sol–gel dip coating method. *Mater Today Proc*. 2020;23:68-72. doi:10.1016/j.matpr.2019.06.651
22. Jabbar S, Asif H, Ahmad R, Sharif S, Khan IA, Shafique MA. Changes in structural and optical properties of TiO_2 thin films irradiated by various doses of 300 keV carbon ions. *J Mater Eng Perform*. 2024;33(12):6014-6023. doi:10.1007/s11665-023-08368-5
23. Kang M, Kim SW, Park HY. Optical properties of TiO_2 thin films with crystal structure. *J Phys Chem Solids*. 2018;123:266-270. doi:10.1016/j.jpcs.2018.08.009